**Title**
Chemotherapy Drug Capture Device Based-on Nanocellulose/ Silk Fibroin Microparticle



**Author**
Sarikhani, Einollah

**Publication Date**
2020

Peer reviewed|Thesis/dissertation

UNIVERSITY OF CALIFORNIA

Los Angeles

# Chemotherapy Drug Capture Device Based-on Nanocellulose/ Silk Fibroin Microparticle

A thesis submitted in partial satisfaction of
the requirements for the degree Master of Science in
Bioengineering

by

Einollah Sarikhani

2020

ABSTRACT OF THE THESIS

Chemotherapy Drug Capture Device Based-on

Nanocellulose/ Silk Fibroin Microparticle

by

Einollah Sarikhani

Master of Science in Bioengineering

University of California, Los Angeles, 2020

Professor Zhen Gu, Chair

Chemotherapy drugs such as a DOX is a common method for cancer treatment. However, severe side effects can limit the administration of these drugs. To ameliorate detrimental side-effects of chemotherapeutic agents, one approach is to implement a capturing device to intake residues of chemotherapy before spreading to the blood circulation. Here we introduced a packed

mesh of Silk Fibroin and Nanocellulose microbeads that can effectively bind to the DOX through negatively charged carboxylic group of ENCC and positively charged nitrogen in DOX. Step emulsification microfluidic device with the scale-up capability used to fabricate homogenous microbeads that were placed into a porous mesh. The represented device can capture 800 μg of DOX with 200μg of microbeads only after two pass flow. In addition, the *in vitro* experiment demonstrates the effect of the SF and ENCC microbeads on NIH-3T3 fibroblast cell on reducing toxicity of DOX.

The thesis of Einollah Sarikhani is approved.

Song Li

Xiaoyu Zheng

Zhen Gu, Committee Chair

University of California, Los Angeles

2020

# ACKNOWLEDGEMENT

Firstly, I would like to thank my advisor Prof. Ali Khademhosseini for his guidance and supports and giving me the opportunity think about the big picture. Also, I also would like to thank my committee members Profs. Zhen Gu, Song Li, And Xiaoyu (Rayne) Zheng for providing me the support feedback, and helping me approach my work from different aspects.

Also, I would like to appreciate the tremendous help of Khademhosseini lab members, Dr. Amir Sheikhi for outlining the work, synthesizing ENCC, revising the writing, and providing scientific input. This work is based on his previous work of Amir Sheikhi on using ENCC for removal of chemotherapy drug. KangJu Lee for synthesizing Silk Fibroin. Reihaneh Haghniaz for taking SEM images and revising manuscript. Petar Antovski for running *in vitro* biological efficiency test of microbeads. Andrew Schimdt for helping me throughout the experiment and revising the manuscript. I would like also to thank Joe de Rutte and Di Carlo lab for providing the microfluidic device.

Finally, I would like to share my love to my family and friends who were always there for me during this journey. My parents and siblings, thank you for your enthusiasm and belief in me. And thanks to my supportive friends, Keyvan, Hamed, Roholamin, Hossein who made this chapter of my life enjoyable

# 1 Introduction

Cancer is the second leading cause of death in United States with more than 500,000 deaths per year. (1, 2) There are many treatments for cancer including surgery, chemotherapy, immunotherapy, radiation therapy, and targeted drug therapy. Among these, chemotherapy is a common choice for primary and/or adjuvant treatment of a variety of cancers. However, chemotherapy can cause toxic systemic side effects due to drug delivery problems such as physical barriers, off-target delivery, and drug resistance. (3-8)

To reduce the reported detrimental side effects of chemotherapeutic agents such as anemia, neutropenia, mucositis, pericarditis, alopecia, vein thrombosis, pain, and hair loss, direct administration of drugs to the tumor via minimally invasive procedures such as trans-arterial chemoembolization (TACE) and intra-arterial chemotherapy (IAC) have been employed. (9) However, excess drug not actively killing cancer cells can pass through the veins to the heart, and in turn enter circulation and cause systemic toxicity.(10, 11)

To address the aforementioned problems and reduce the systemic toxicity of chemotherapy, an intravenous drug capturing device for absorbing residual chemotherapy can be employed before spreading chemotherapeutic agents such as Doxorubicin (DOX) into systematic circulation. Having such a device in place can lead to more efficient targeted chemotherapy as it would allow oncologists to prescribe higher doses combined with less toxicity, effectively reducing the dose-limiting effect of doxorubicin. (10, 12, 13) There have been efforts towards making such a device for capturing DOX. Patel et al. designed and developed a chemotherapy filter for intra-arterial absorption of doxorubicin with the help of ion-exchange resins. They have reported capturing of 52% of DOX solution in the flow test study within first 10 min and 80%

capturing after 30 min from 50 mg DOX injected.(10) In another study, Blumenfeld et al. reported DNA-coated iron-oxide nanoparticles that demonstrated the ability to capture three chemotherapy agents: DOX, cisplatin and epirubicin. 100 mg of these DNA-functionalized magnetic particles can capture up to 93% of 1 mg DOX from porcine blood. Additionally, cytocompatibility study of rat cardiac myoblasts H9C2 cell line evaluated in the presence of functionalized magnetic particle, which demonstrated the reduce toxicity level of DOX(12). Recently, Hee Jeung Oh et al. designed a 3D printed porous structure coated with a block copolymer that includes sulfonate groups as the capturing agent. Results of this study demonstrated that their structure could absorb up to 64% of 50 mg DOX from circulation in swine *in vivo* models. (10, 13, 14)

Here in this study, we introduced a novel drug capturing device (DCD) as a promising method for intravenous absorption of DOX. We have tested the device *in vitro* to evaluate the efficiency of the device for DOX capturing. The capturing ability of the device come from Silk-Fibroin (SF) microparticles fabricated with hairy electrosterically stabilized nanocrystalline cellulose (ENCC) using a step emulsification microfluidic device. (15-17)ENCC consists of anionic groups that can bind to the DOX molecules through electrostatic interaction of positively charged nitrogen in DOX and negatively charged groups in ENCC such as carboxylic groups. Microparticles placed into a porous nitinol mesh and can successfully absorb DOX in a flow test study. The presented device can be placed in hepatic vein to at venous outflow to absorb the chemotherapy agent going into the IVC.(18) Also in this study, we investigate the efficacy of our proposed DCD for *in vitro* evaluation of device efficiency for capturing DOX investigated. Also, biocompatibility of microbeads assessed using NIH-3T3 murine fibroblast cell line.

In the Error! Reference source not found., the summary of this work presented as shown here.

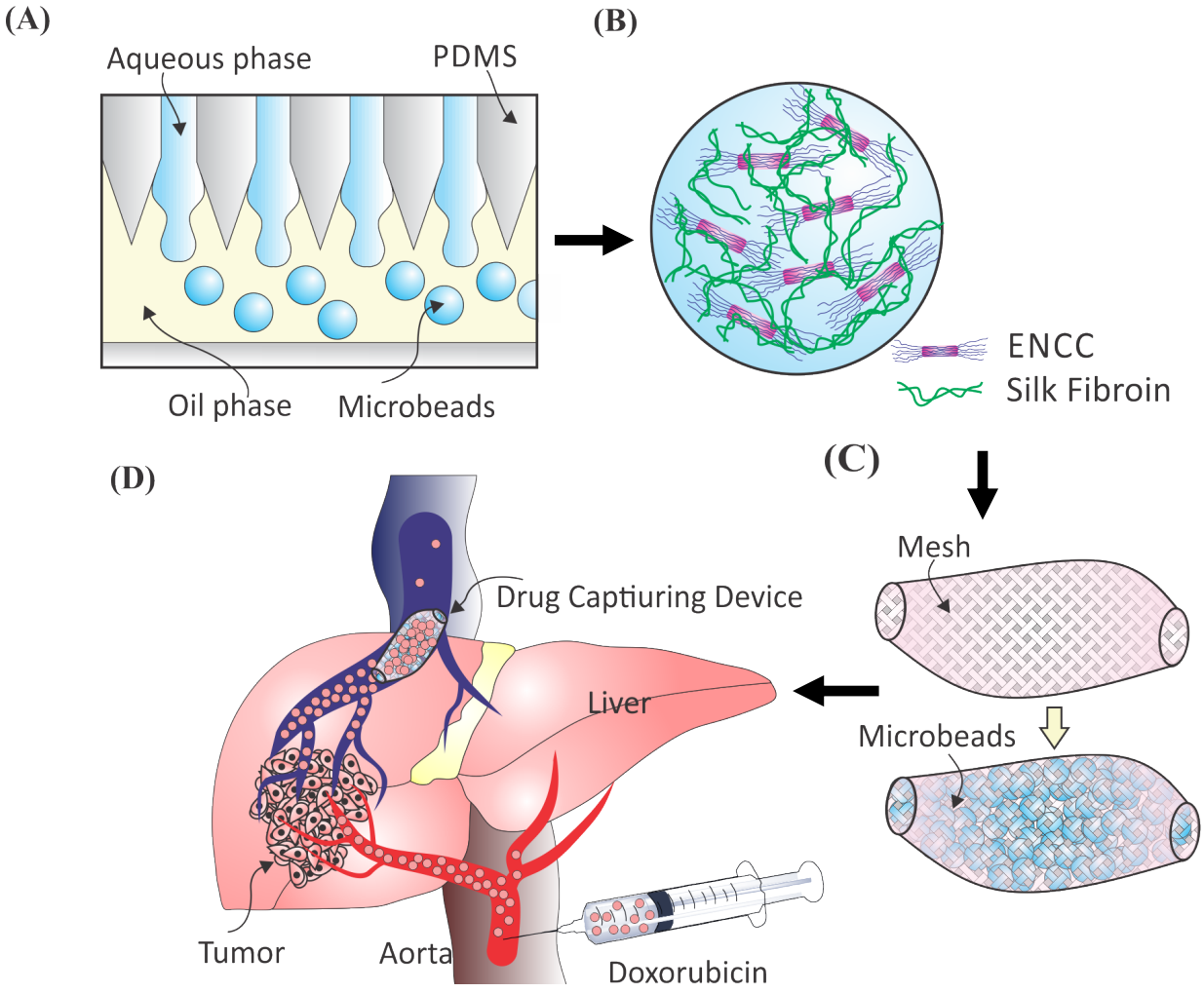


Figure 1. Schematic of the study. Fabrication of homogenous microbeads consist of hairy nanocellulose and silk fibroin. Step-emulsification microfluidic device fabricate microbeads on in the oil phase in the presence of pico-surfactant. Fabricated microbeads after stabilization process placed in a porous mesh. Finally, the efficiency of microbeads-loaded mesh device evaluated to absorb dox in static and dynamic condition. Device is designed to place into venous artery and capture doxorubicin that are in outflow of the venous flow.

## 2 Materials and Method:

### 2.1 Materials:

Silicon wafers were acquired from University Wafer (MA, USA), negative photoresist KMPR 1050 was acquired from MicroChem Corp (MA, USA), and polydimethylsiloxane (PDMS) base and its curing agent (SYLGARD™ 184 Elastomer Kit) was purchased from Dow Corning (MI, USA) were used to fabricate the microfluidic chips. Tygon Flexible Plastic Tubing 0.02" ID x 0.06" OD from Saint-Gobain PPL Corp. (CA, USA) and 1569-PEEK Tubing Orange 1/32" OD x .020" ID from IDEX Corp. (IL, USA) were used with the microfluidic device. 3M™ Novec™ 7500 Engineered Fluid (Novec 7500 oil) was provided by 3M (MN, USA). Pico-Surf™ 1 (5% (w/w) in Novec™ 7500 was purchased from Sphere Fluidics Inc. (Cambridge, UK). For the fabrication of silk fibroin, *Bombyx mori* cocoons were from Uljin Nongwon, South Korea were acquired. Sodium oleate (KANTO Chemical Co., Japan) and $Na_2CO_3$ (DAEJUNG Chemical & Metals Co., South Korea) were used to boil the cocoons. Lithium bromide was provided by SAMCHUN Chemical (South Korea). Dialysis membrane with 14,000 kDa molecular weight cutoff (MWCO) was provided by Sigma Aldrich (MO, USA). Formic acid purchased from Fisher Scientific (PA, USA).

Doxorubicin hydrochloride powder was from Oakwood Chemical (SC, USA). ENCC was made from NCC in water (15.6 mg/ml) and DCC in water (7.4 mg/ml) provided by Thermo Fisher Scientific. Milli-Q water with an electrical resistivity of 18.2 MΩ cm at 25 °C was purchased from Millipore Corporation Dulbecco's phosphate-buffered solution (DPBS) free of calcium and magnesium was also provided by Gibco (NY, USA) (pH 7.3). Bovine serum albumin (BSA) was from Sigma Aldrich (MO, USA). Silicone tubing with 3.1 mm inner diameter (ID) and 1.6mm wall thickness for the flow test was provided by Longer Precision Pump.

## 2.2 Fabrication of microfluidic device:

A step emulsification device was fabricated using soft lithography. Briefly, 4inch mechanical grade silicon wafers were coated with 80 and 70 μm layers of negative photoresist (KMPR 1050) and patterned in sequence using standard photolithography techniques. PDMS base and the curing agent were mixed at a ratio of 10 to 1, poured onto the molds in petri dishes, degassed, and cured in an oven at 65 °C for at least 4 h. The PDMS device was peeled from the mold and punched with 0.8 mm holes at the inlets and outlets. Devices and glass slides were then activated via air plasma (Plasma Cleaner, Harrick Plasma, NY, USA) and bonded together to enclose the microchannels. The devices were then treated with Aquapel and subsequently washed with Novec 7500 oil to make channel surfaces fluorophilic. (16, 19)

## *2.3* Silk Fibroin Purification:

Silk fibroin synthesized and purified as previously described.(20, 21) Briefly, *Bombyx mori* cocoons were degummed to remove sericin, waxes, and other impurities. The cocoon was boiled in an aqueous sodium dodecylsulfate (0.25 wt%) and sodium carbonate $Na_2CO_3$ (0.25 wt%) solution for 1 h at 70° C. The degummed silk was then dissolved in a 9.3 M Lithium bromide (LiBr) solution. The silk fibroin-LiBr solution was dialyzed against deionized water in 3500 Da dialysis tube for at least 3 days to remove excess LiBr. The resultant silk fibroin-water solution was lyophilized and stored at -80 °C for future use.(21, 22)

### *2.4* Synthesis of ENCC:

ENCC synthesized through two step process consist of periodate oxidation and chlorite oxidation(17). For the periodate oxidation, 1 mg of softwood kraft pulp soaked in water and rigorously mixed to ameliorate the fiber disintegration. Vaccum filtered pulps reacted with 200 ml of water with 0.66 g $NaIO_4$ and 3.87 g NaCl for 4 days at room temperature. Fibers washed with DI water, filtered and resuspended at 80 °C for 6 h.(17, 23) Chlorite oxidation process starts with suspending 1 mg of modified pulps of periodate oxidation in water containing 3.56 g $NaClO_2$ and 14.6 g NaCl. 3.3 g $H_2O_2$ added to the solution and stirred at room temperature and 105 rpm for 24 hours, while pH maintained at 5 by adding NaOH. Mixture centrifuged after adding ethanol that can precipitate ENCC. (17, 24, 25)

### 2.5 Microbeads Fabrication and Characterization:

The lyophilized SF was dissolved in 99.0% formic acid at varying concentrations (1-3 % w/v). SF was used as the structural component of the microbeads. Varying concentrations of SF and ENCC were used to generate microbeads with a variety of characteristics to optimized system for maximal DOX capturing. SF dissolved in formic acid and stirred at 100 rpm for 1d to dissolved uniformly. ENCC with 7.2 v/v % concentration added to yield final solutions with concentrations displayed in *Table 1.* Step emulsification microfluidic chip designed to produce 100 μm beads through hundreds of channels from aqueous solution. SF solutions were filtered through a 20 μm filter to prevent channels from clogging. solution heated to 37°C (to decrease viscosity) before injection into the chip. SF solutions were used as the aqueous (dispersed) phase in the microfluidic device. A Novec 7500 oil-surfactant (0.5 wt% PicoSurf) mixture was used as the oil (continuous)

phase. The solutions were injected into the chip using syringe pumps (Harvard Apparatus PHD 2000, MA, USA) to form surfactant-stabilized SF or SF-ENCC microbeads. The flow rates for the aqueous (dispersed) and oil (continuous) phases were optimized for each SF solution in order to generate homogenous beads before collecting samples. The bead suspension samples were collected in microcentrifuge tubes.

### 2.6 Microbead stabilization:

After collection, each sample of beads was allowed to settle and phase separate for at least 15 minutes. Excess oil-surfactant solution was removed from the bead-oil suspension, leaving behind just enough oil to maintain stable beads. Methanol (5 ml) was added to each sample to crystallize the microbeads resulting in SF microbeads consisting of β-sheet structure. The beads were then transferred to 15 ml conical tubes and centrifuged at 2000 rpm for 3 min, and vortexed for 15s.This process repeated at least 5 times to make beads completely crystalized. Excess methanol from the supernatant was removed and the beads were transferred into a clean microcentrifuge tube using positive displacement pipette (MICROMAN® E, Gilson, WI, USA) back into a clean microcentrifuge tube. DPBS was added to the beads to test their stability in aqueous solution at 25 and 37 °C.

### 2.7 Time-dependent DOX capturing experiments:

Time-dependent Dox capturing experiments were performed with microbeads that were collected until 30 µl of the aqueous phase was passed through the chip and into the microcentrifuge

tube. Each sample was treated with methanol as stated above for crystallization of silk(21). The crystalized beads were transferred to a microcentrifuge tube via pipette before adding the DOX solution. 250 µl of 1.0 mg/mL Dox in 35 mg/ml BSA in DPBS was added to each sample for this experiment. DOX concentration measurements were taken at various time points throughout the first hour. At each timepoint, the sample was spun down and a 2 µl aliquot was removed to measure the DOX concentration of the supernatant. The sample was then vortexed after the aliquot was removed. The DOX concentrations were measured with a UV-Vis Spectrophotometer (NanoDrop OneC Thermo Fisher Scientific (MA, USA)) at 480 nm wavelength.

### 2.8 SEM Imaging:

Morphology and porosity of the microbeads were visualized using scanning electron microscope (SEM, Supra 40 VP, Zeiss, Germany). Microbeads were crystalized with mentioned procedure and sputter-coated (IBS/e, ion beam sputter deposition and etching system, South Bay Technology, CA, USA) with iridium. SEM images were obtained at 10 and images analyzed using ImageJ (Version 1.52e, National Institute of Health, USA).

### 2.9 Time-dependent Dox release experiment:

Release study of beads after capturing was performed by adding the beads after static DOX removal study (conditions described in **Section 3.6**.). After removing the supernatant of the static capturing test .1mL of 35 mg/mL BSA in DPBS was added to microbeads that absorbed DOX. Subsequently, measurements of the DOX concentration were taken over an hour after vertexing

the solution with microbeads.

### 2.10 Microscopic fluorescence imaging:

To demonstrate that the fabricated microbeads can capture DOX and retain them in their structure, crystalized beads were collected and imaged before and after static DOX capturing test. Fluorescent signal was monitored using fluorescence microscope (Zeiss, Germany) under Alexa flour channel at excitation/emission wavelengths of 568/603 nm.(26, 27)

### 2.11 DOX capturing flow experiment:

For the Dox capturing flow test experiments, particles were collected until 150 µl of the aqueous phase was passed to the microfluidic chip. Crystalizing the beads carried out by the abovementioned method. Beads were added to the mesh and sealed with glue in order to prevent leakage of beads out of the mesh structure. 5 mL of DOX solution with the concentration of 0.25 mg/mL was pumped through the mesh and beads with a peristaltic pump at 18.84 ml $min^{-1}$. The inner diameter of the plastic tubing was 3.1 mm. Dox concentration of the filtrate was measured with the NanoDrop OneC at the wavelength 480 nm.

### 2.12 Dox Capturing Biological evaluation:

First, we prepared the DOX solutions by adding 400 µg/ml DOX into the fibroblast cultured media). Media prepared with Dulbecco's Modified Eagle's medium (DMEM)

supplemented with 10% fetal bovine serum (FBS) and 1% Pen-Strep or complete HUVEC media correspondingly. There were 3 different ENCC microbead test groups 1x, 2x and 5x. The names refer to the amount of microbeads added to each test well. For example, 1x contained the amount of beads that was showed to remove all of the DOX from a 200 µl 400 µg/ml Dox PBS solution. 2x and 5x contained 2 times and 5 times of that amount of microbeads correspondingly. The microbeads were thoroughly rinsed in DPBS 3 times before being used for the cell experiment. For the ENCC microbead treated samples we added 200 µl of the DOX and media solution to the microbeads in each well. The mixture was thoroughly mixed by vertexing it for 30 seconds, incubated for 5 minutes and then centrifuged at 1000 rpm for 1 minute. From the supernatant 100 µL were added to the bottom compartment of the corresponding test wells. The remaining supernatant was used to resuspend the microbeads and then added to the top compartment of the corresponding test wells. To determine the effect of ENCC treatment on cells, 5000 3T3s were seeded in the bottom compartment of a 96 transwell plate with 200 µl prepared HUVEC media. The cells were left to attach to the bottom of the wells overnight. The next day the media was aspirated, the cells were rinsed with 200 µl phosphate buffered saline (PBS) and then to the bottom compartment 100 µl of 3T3 culture media was added in the control group wells, 100 µl of the supernatant from each microbead treated sample was added to the corresponding microbead group wells and 100 µl of the 400 µg/ml DOX media solution was added to the DOX group wells. Then to the top compartment 100 µl of 3T3 culture media was added in the control group wells, the remixed microbead solution, containing the microbeads, was added to the corresponding microbead group wells and 100 µl of the 400 µg/ml Dox media solution was added to the DOX group wells. Each group consisted of 5 wells. After 8 hours, the media was aspirated, the cells were rinsed twice with 200 µl PBS and then 100 µl of PrestoBlue reagent (Thermofisher) was

added to each well. The cells were incubated for 45 minutes and then the PrestoBlue absorbance was recorded using a fluorescence microplate reader (vis Synergy 2, BioTek). Immediately afterwards, the cells were again rinsed 2 times with 200 µl PBS and then 150 µl of LIVE/DEAD reagent (Thermofisher) was added to each well following the manufacturer's protocol. The cells were incubated for 90 minutes and then fluorescent images were taken. The fluorescent images were analyzed using ImageJ Software to quantify the number of live cells.

### 2.13 Statistical Analysis:

All results are presented as means ± standard deviation of the mean (SD). Comparison of treated and untreated beads and flow study made by unpaired t-test. *In vitro* capturing study experiment and release study of beads were analyzed and compared using ordinary one-way analyses of variance (ANOVAs) with three replicates (n=3). Biological efficiency of beads was analyzed one-way ANOVA with six replicates (n=6). For all statistical tests, the level of significance was set at $P<0.05$.

# 3 Results and Discussion:

## 3.1 Microbead stability:

A step emulsification device as shown in **Figure 2** designed to fabricate uniform microbeads from silk fibroin with high efficiency and scalability.(16, 28) Formic acid with varying concentrations of dissolved SF constituted the aqueous (continuous) phase. The aqueous phase flowed toward channels that connected to the continuous oil phase containing Novec oil and Pico surfactant with concentration of 0.5%.(29) Expansion of channel height at the end of each channel results in forming the single bead into the continuous oil phase (**Figure 3A**). Droplet forms in step emulsification depends on the viscosity of aqueous phase.(30, 31) Considering the viscosity of the aqueous phase the flow rate of both oil and aqueous phase adjusted to make the uniform microbeads. Flow rates used for aqueous phase is 10-20 mL/ min for aqueous phase and 50-100 mL/ min for the oil phase depending on the viscosity of the aqueous phase. Microbeads diverse in the continuous oil flow, collected from the reservoir of the device as shown in **Figure 3B, C.**

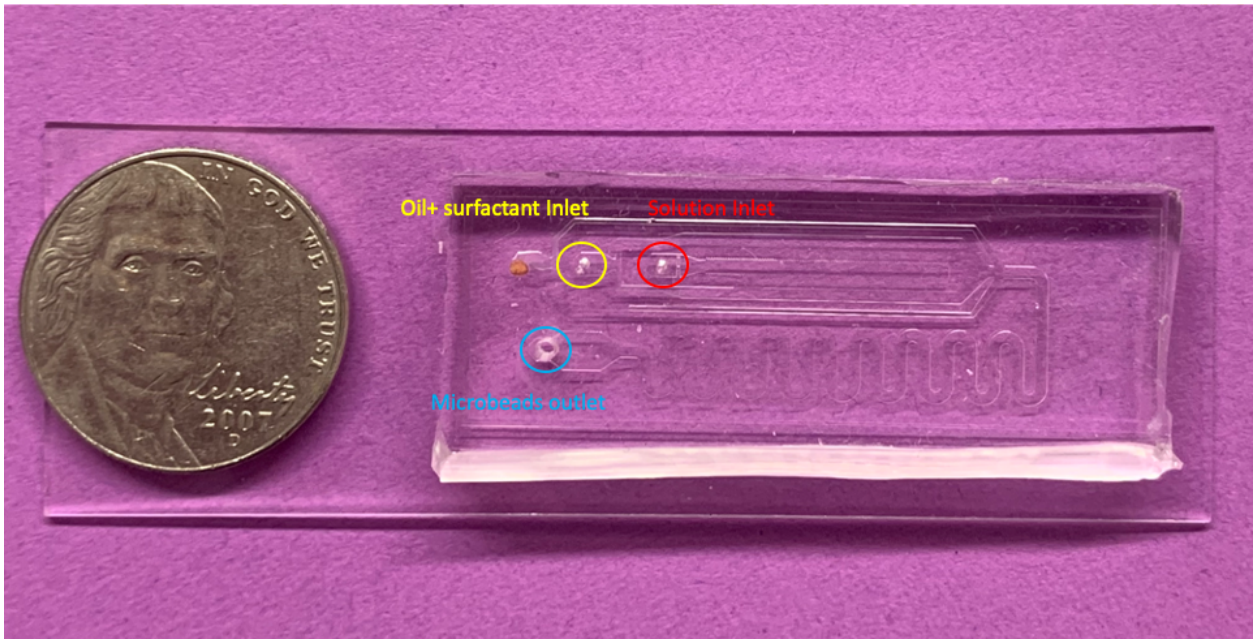


Figure 2. image of step emulsification microfluidic device comprising an inlet for the aqueous phase of Silk fibroin and ENCC, continuous flow (oil/surfactant) inlets, and outlet for collecting microbeads. The fabricated beads were monitored in oil reservoir and collected for further washing and crystallization.

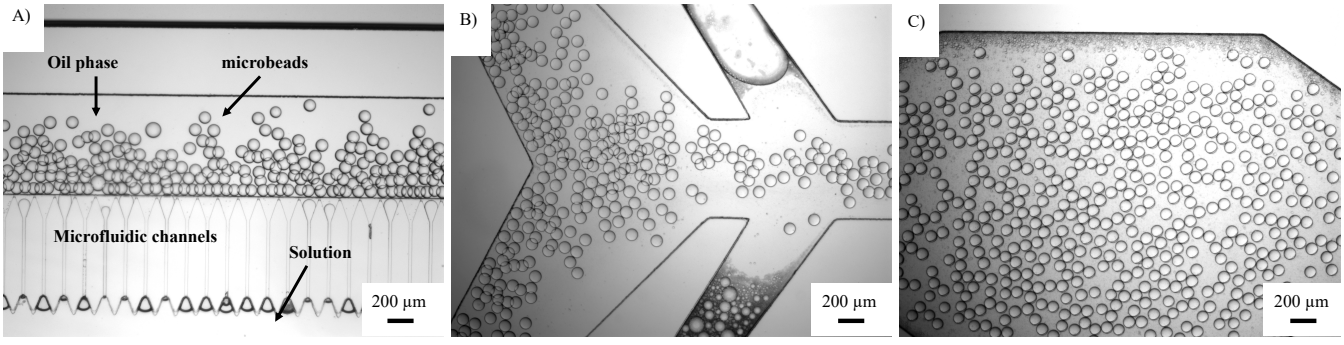


Figure 3. Fabrication of microbeads into the oil phase upon expansion of the channel, collection of microbeads and microbeads in oil reservoir.

To further study of the microbeads and using them as the capturing material we implemented methanol treatment to stabilize and crystallize the microbeads.(21, 22, 32) Methanol treatment of SF material accounted for increasing the stability of SF materials due to β-*sheet* formation. After removing the oil phase from the sample collected from the device microbeads were crystalized by the methanol treatment as shown in **Figure 4A**.(21, 33)

To investigate the stability of the beads for the drug capturing device, microbeads were transferred to the 1X DPBS solution. As demonstrated in the **Figure 4B** microbeads are able to maintain their round shape and size in 1X DPBS solution, after treated with methanol with aforementioned method. The beads with 3% (w/v) SF and ENCC were generated with the average size of 77.01 ± 13.32 µm at optimized flow rates which is 15 mL/min. Crystalizing beads with methanol and suspending beads into DPBS slightly increased the average size of beads to 100.04 ± 20.20 µm. (**Figure 4C**)

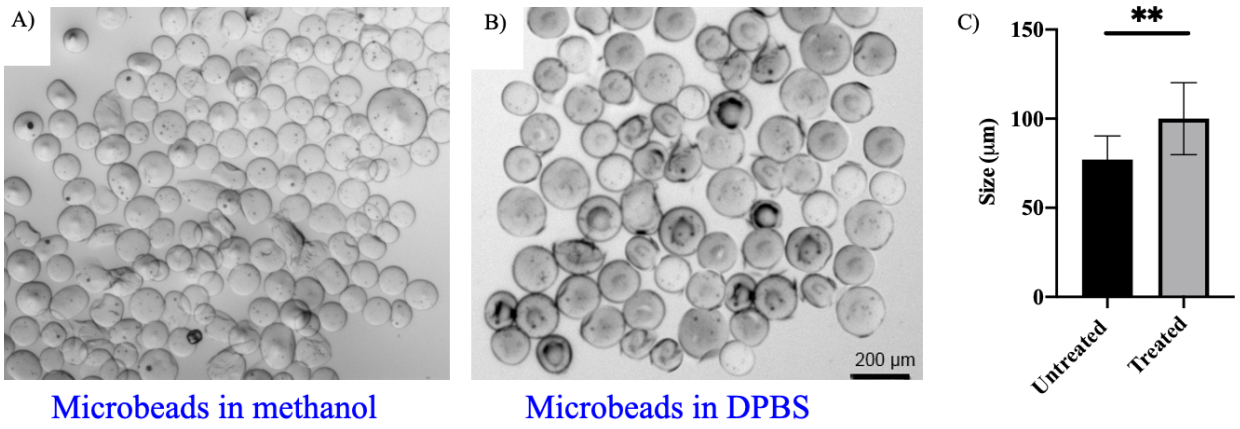


Figure 4. A) Image of microbeads with methanol treatment to form $\beta$- sheet. B) suspension of microbeads in DPBS. (C) Silk Fibroin beads size (untreated beads show average size of 77.01 ±

13.3 while crystalized beads show the average size of 100.04 ± 20.20).

To achieve the idea of having microbead-loaded mesh as the structure for carrying capturing agents we used a Nitinol mesh from Monarch Bio (CA, USA) with fine structure Figure 5**A, B**. The mesh exploit as a supporting structure to keep the beads from spreading to the blood flow. Pore size of the mesh (Size of pores) is smaller than microbeads size which impeded the beads spreading out of the mesh. On the other hand, porous structure of mesh to allows flow go through the mesh with the beads without clogging. To scrutinize this idea, crystalized microbeads added to the mesh and imaged from bottom to show the beads inside the mesh and compare the beads size and pores of the mesh. As shown in **Figure 5C** beads on the top of mesh structure demonstrate that the microbeads can be entrapped inside the mesh because of their size and the mesh is able to hold the beads without releasing them.

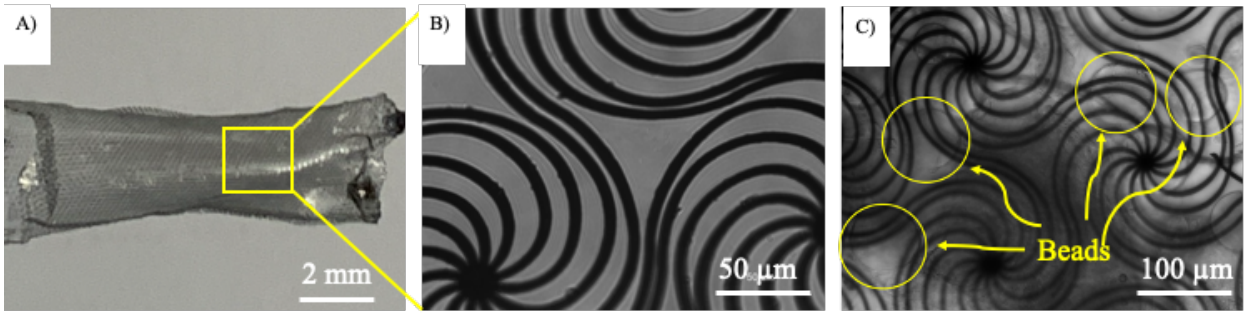


Figure 5. A) Macro and B) microscopic images of mesh and images of beads inside the mesh. (C) Image of beads entrapped inside the mesh. Pore size of the mesh shows are smaller than beads size which prevent beads from flowing outside of the sealed mesh.

### 3.2 In vitro testing of the microbeads in DOX solution:

In order to evaluate the efficiency of SF and ENCC based microbeads to absorb DOX as a chemotherapy agent from the solution we studied the static condition with the DOX solution in DPBS and BSA (35 mg/mL) with various fabricated beads. Results of static capturing study of DOX reveals the effect of both ENCC and SF concentrations in capturing the DOX. Interestingly, both of the SF and ENCC effectively could absorb the DOX molecule. Nitrogen group in DOX can be protonated and make DOX positively charge which can be bind to the negatively charged groups in ENCC and SF via electrostatic forces.

In the microbeads with 3% (w/v) SF as shown in **Figure 6A** with the increase in ENCC amount the DOX capturing capacity significantly increased from 26% to 68% of the 1 mg/mL solution. The amount of DOX captured by the same amount of beads increased from 0.068 mg DOX to 0.162 mg DOX, which shows significant increase in the efficiency of beads as a capturing material. In addition, ENCC can significantly boost the efficiency of the beads which makes it promising capturing agent for the application of drug capturing devices. Also, Image of solutions after capturing visually confirms the capturing capacity of each group as shown in **Figure 6B**.

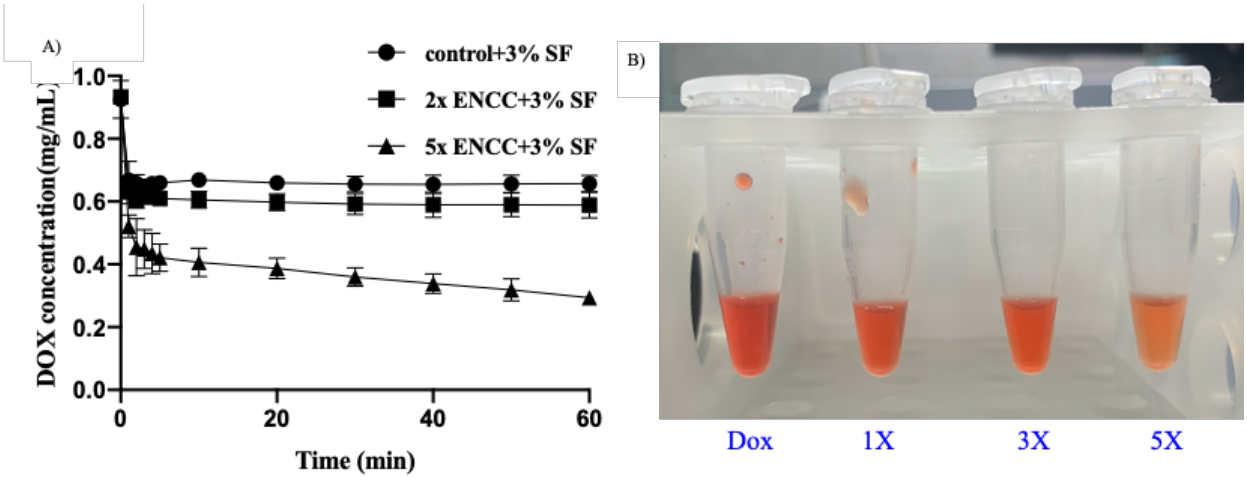


Figure 6. (A) Doxorubicin concentration function of time in the presence of 3% w/v silk fibroin beads and various amounts of ENCC. (B) Represented image of solutions after capturing which qualitatively confirms the dox concentration quantitative data.

Also, **Figure 7A** shows the capturing capacity of 1% w/v silk fibroin-based microbeads varying amount of ENCC. As results show in the 1% w/v SF similar to 3% w/v SF microbeads, ENCC improved the capturing capacity. **Figure 7B** compares the solutions color where the darker color accounted for more concentration of dox. Qualitative image of solutions shows consistency with the quantitative plot represented in **Figure 7A.** Comparing the amount of DOX captured between 3% SF and 1% SF demonstrate that there is not significant difference between two types of beads indicating that SF reached to the maximum capacity of absorbing DOX. Static study of microbeads shows that the beads can reach to the 64% and 80% of their capacity just after respectively 1 and 5 minutes, respectively. While due to scalability of beads production with the step emulsification device the amounts of beads can be controlled to achieve desired absorbed DOX amount. The optimal ratio of ENCC (5x) were selected after we tested 25x ENCC which

demonstrated no increase in the amount of DOX captured (0.164 mg).

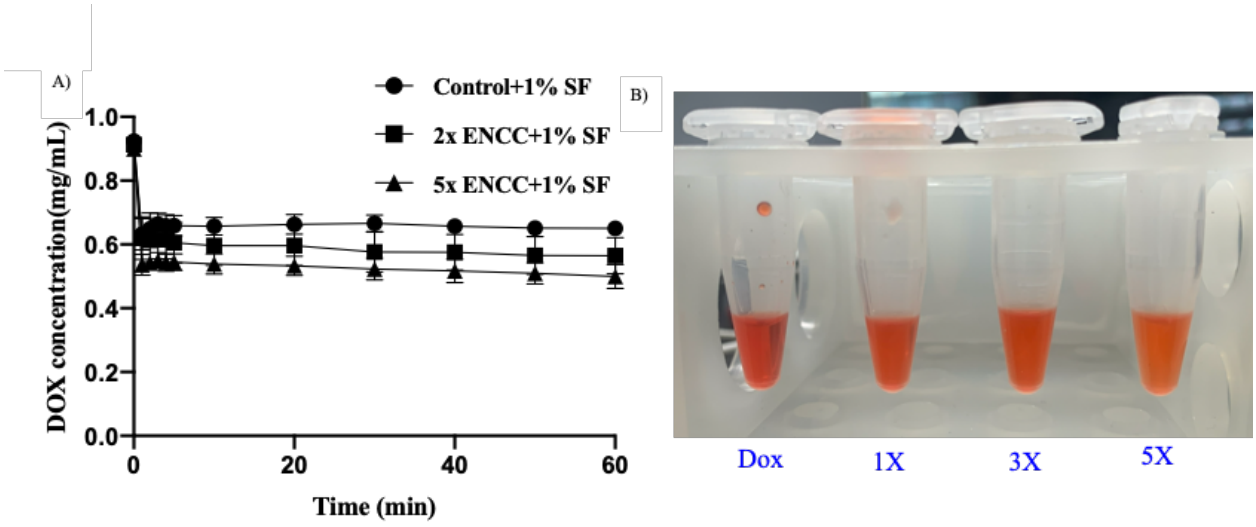


Figure 7. (A) Doxorubicin concentration function of time in the presence of 1% w/v silk fibroin beads and various amounts of ENCC. (B) Represented image of solutions after capturing which qualitatively confirms the dox concentration quantitative data.

To better understand the DOX capturing capacity of 3% w/v SF beads, the results were compared to each other as shown in **Figure 8A.** The capturing capacity of microbeads demonstrates that adding ENCC to the silk fibroin solution can significantly enhance the capacity for drug absorbance compare to the control sample. After static *in vitro* capturing experiment, we tried to perform release study of dox from microbeads by vertexing beads transferred to the 1X DPBS solution. Analyzing the solution over 1 h in **Figure 8B** showed less than 10% (9.20 ± 1.89) of DOX released over the mentioned period of time in harsh vertexing condition, which indicates that DOX can bind to the microparticles strongly.

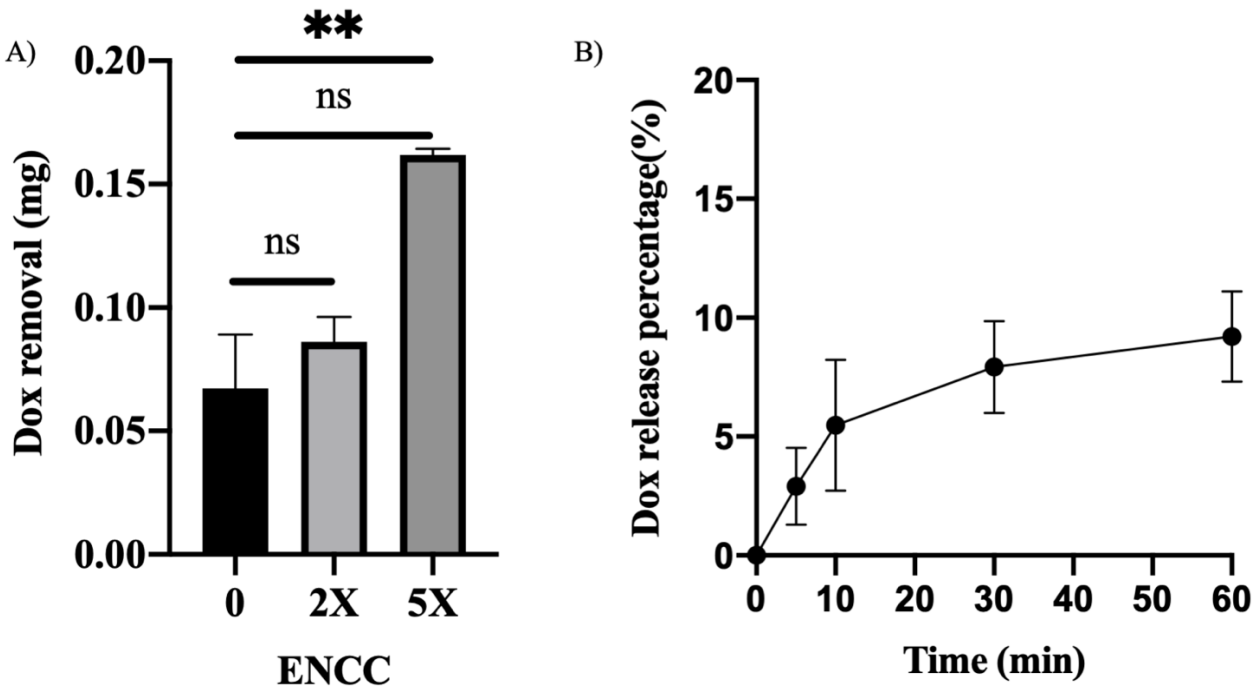


Figure 8. A) comparison of amount of DOX captured by 30 mg of 3% silk fibroin beads which shows 3% SF with 5X ENCC can capture .167 mg of DOX form the solution. B) Release study of the microbeads 3% SF and 5X ENCC showed 2.92± 1.69 % release after 5 mins, 5.46± 2.76 after 10 mins, 2.92± 1.69 % after 30 mins and %9.20 ± 1.89 % release over 1 h.

To further confirm the binding of DOX to the microbeads and capturing verification SEM imaging performed with the 3% w/v and 5X ENCC microbeads, before and after capturing study. **Figure 9A** illustrates the round shape of beads with the ENCC and SF on the surface after crystallization and before capturing study. The structure of beads and presence of functional groups on the surface of the beads justify their ability to bind to the DOX molecules. **Figure 9B,** on the other hand shows the binding and presence of DOX on the surface of microparticles.

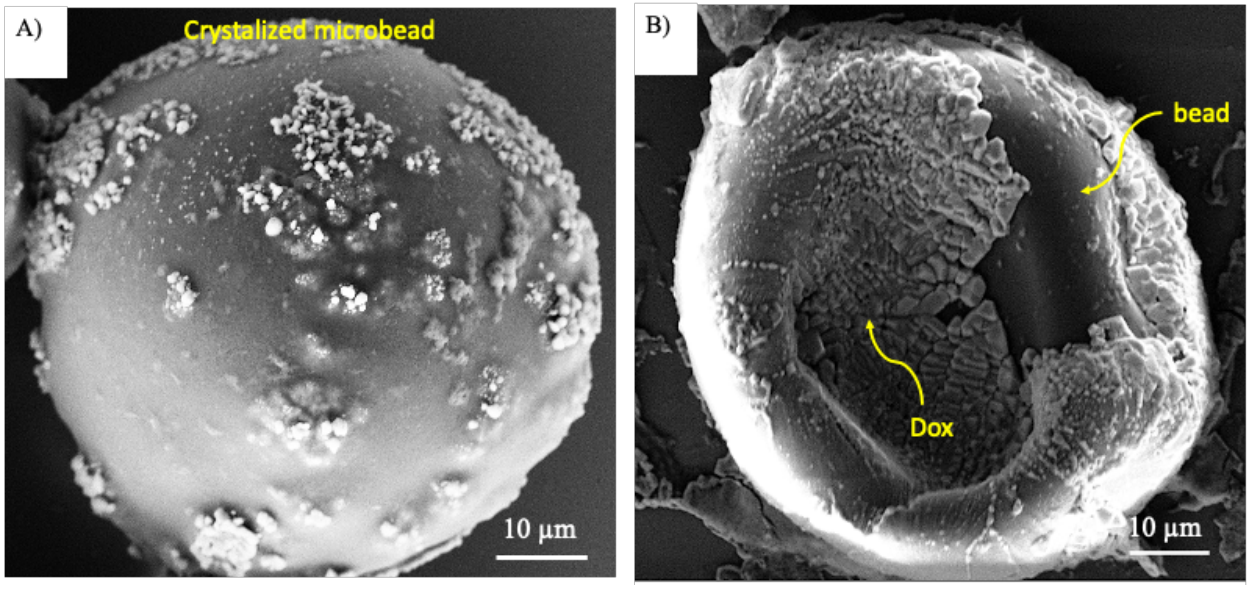


Figure 9. A) SEM images of crystalize microbead before capturing. B) image of microbead and Dox absorbed after capturing study.

Fluorescence microscopy performed to visualize the absorbance of binding DOX to the microbeads. In this order, Fluorescence microscopy of crystalized microbeads before and after capturing showed in the **Figure 10A and Figure 10B** respectively. **Figure 10A** demonstrates the lack of fluorescent properties of beads before DOX capturing study. However, as shown in **Figure 10B,** which is related to the fluorescent image of microbeads after capturing experiment, particles transferred to the 1X DPBS solution imaged with fluorescent microscope displayed the binding of DOX to the beads after removing beads from DOX solution.

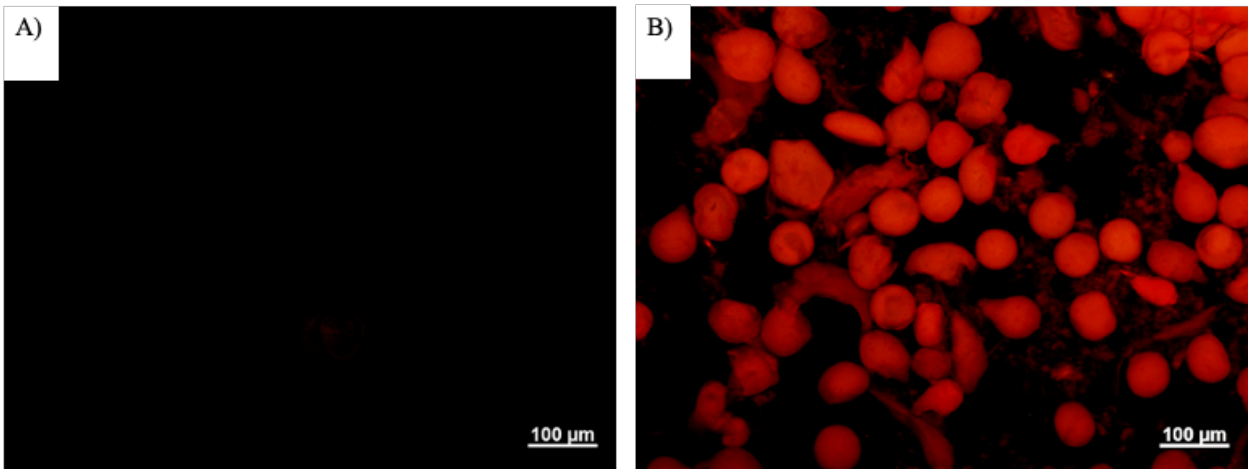


Figure 10. A) Fluorescent images of microbeads used for the device before capturing Dox and B) after capturing Dox.

For the dynamic *in vitro* evaluation of our drug capturing device, the abovementioned mesh filled with microbeads equivalent to 200 uL of solution and sealed carefully. The mesh was placed in a tube with 3.1 mm diameter to mimic the rat model blood flow with the flow rate of 18.84 mL/min. DOX solution in DPBS and BSA used as a sample in a syringe and heated up to 37 C to simulate the physiological condition. The fluid was continuously flowed through the tubing in the setup shown in **Figure S1** and concentration of solution measured after each pass of whole fluid through the mesh. Results of dox absorbed by the mesh beside visual clearing of the dox solution after each time pass present in **Figure S1B**. Results show that the device can capture 0.8 mg of 1 mg DOX after two passes of flow through the mesh. Harvesting the mesh after flow capturing study can visually confirm the dox absorbance by the change in the color. In addition, mesh could keep its shape after preforming the flow test without clotting the tube.

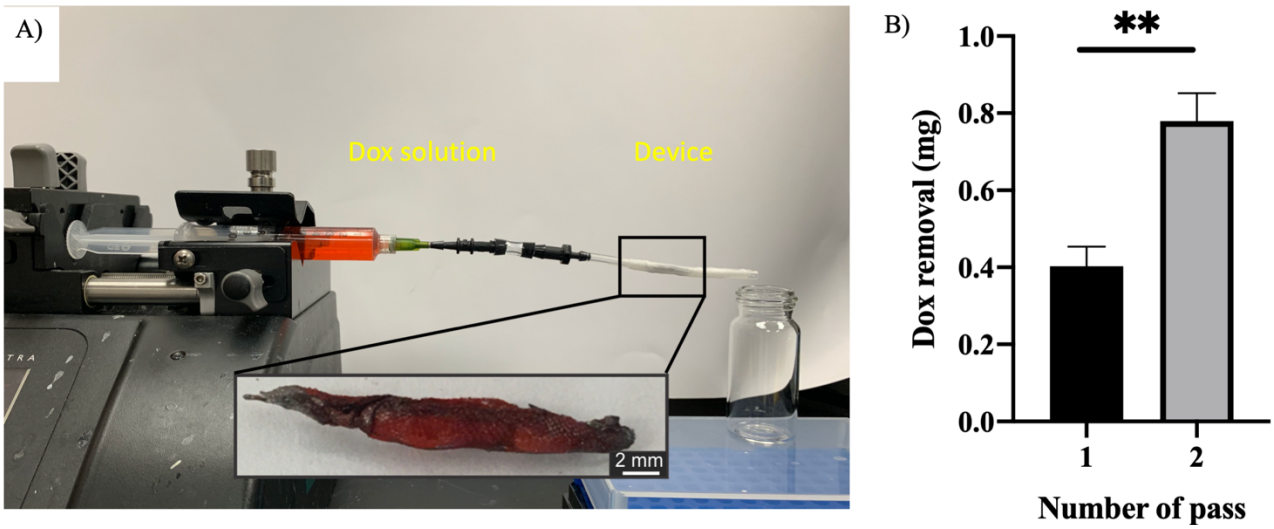


Figure 11. (A) Flow experiment setup with the mesh inside the tube and close-up of the microbead-loaded after capturing test. (B) Mass of Dox captured by the beads against number of passes. (n=3)

### 3.3 In vitro biological efficiency of microbeads:

To determine the efficiency of the SF and ENCC microbeads DOX capturing ability in a biological setting we assessed their effect on 3T3 fibroblast cell viability *in vitro*. We performed the experiments using 3 different amounts of selected microbeads (SF with 5X ENCC). Namely, we used 1x, 2x and 5x amount of beads, where 1x is the amount of microbeads that successfully removed all of the DOX from a 200µl of a 400 µg/ml DOX solution in PBS. The microbeads were added to the 3T3 cell culture medium and incubated for 5 minutes before being centrifuged for 1 minute. The supernatant was then added directly to the cells and the resuspended microbeads were added in the separate compartment of the transwell to avoid contact between the cells and the microbeads. The cell viability was assessed by 8 hours using the PrestoBlue assay and the Live Dead assay.

The microbead test groups exhibited a much higher cell viability, shown by the Live Dead microscope images in Error! Reference source not found.**A**. Quantitatively the 1x, 2x and 5x microbead test groups had an average normalized cell viability of 76.65%, 76.25% and 94.46% accordingly, while the DOX only test group had an average normalized cell viability of 28.45% (Error! Reference source not found.**B**). The Prestoblue assay results confirmed the Live Dead assay results as the microbead treatment significantly increased the cell viability, with the microbead test groups having an average normalized Prestoblue absorbance of 71.66%, 72.67% and 83.64% and the DOX only group having an average normalized Prestoblue absorbance of 32.4% (Error! Reference source not found.**C**).

While the capturing efficiency tests carried out in PBS showed that the 1x microbead group is capable of removing all of the DOX from the solution, in our cell experiments we determined

that amount of beads does not remove all of the DOX from the cell culture media and as a result the cell viability is 76.65%. Increasing the amount of microbeads by fivefold increases the cell viability up to 94.46%. This cell viability might be further increased if the solution was not stagnant and the DOX containing solution was flowed through the abovementioned mesh containing the microbeads.

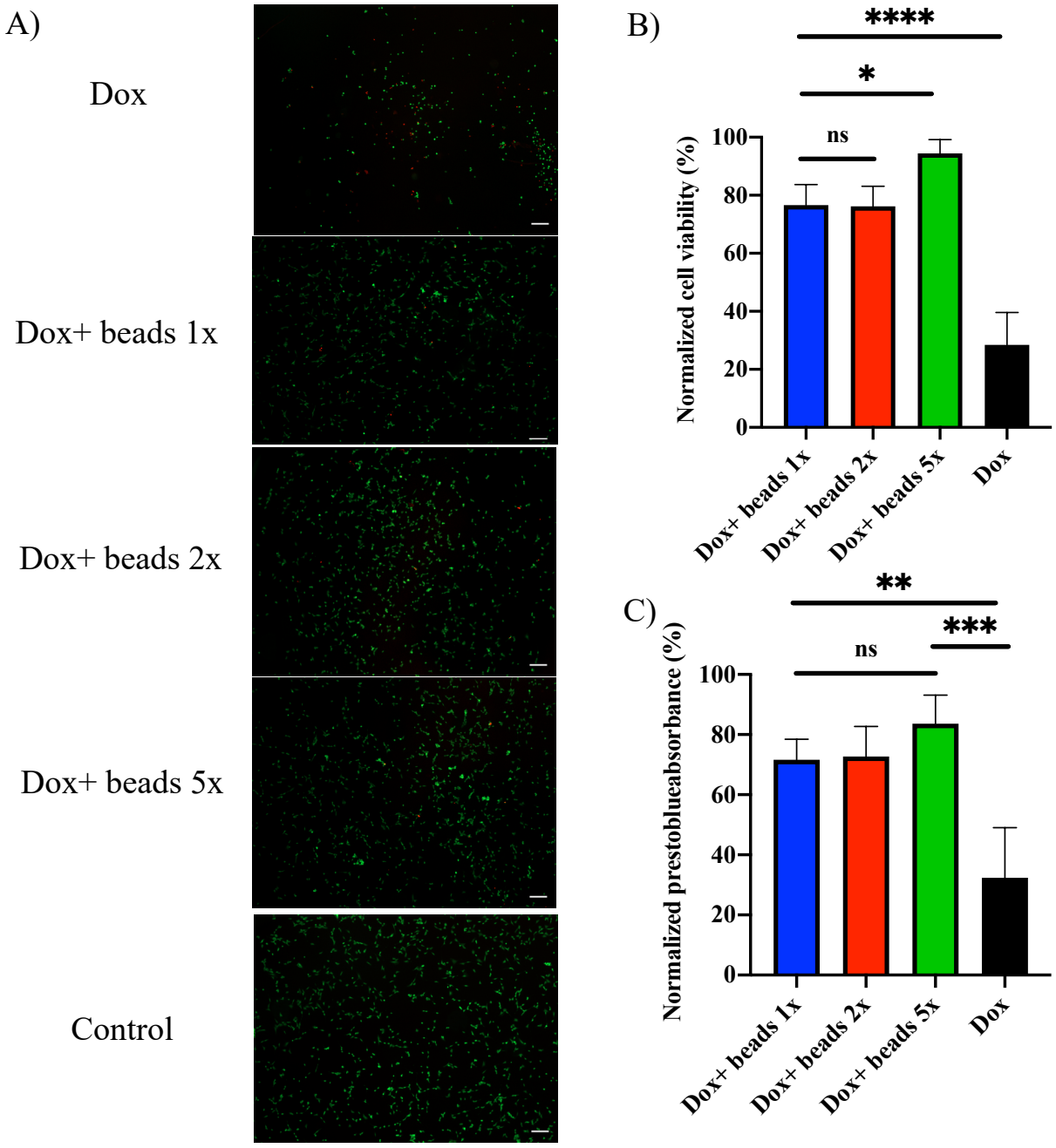


Figure 12. *In Vitro* effect of Dox capture by ENCC containing microbeads on 3T3 fibroblasts A) Live-dead assay images obtained at 8 hours post treatment (scale bar= 200 µm) B) Quantification of live cells from the live-dead assay image. C) PrestoBlue absorbance measured at 8 hours.

# 4 Conclusion:

DCD device designed and tested *in vitro* to capture residual of chemotherapy drug before entering body circulation to reduce side effects of DOX. Microfluidic device with step emulsification method were employed to generate homogenous microbeads with average size of 77.01± 13.3 containing SF and ENCC. Microbeads incorporated inside a porous mesh that allow them to interact with DOX and bind to the DOX. Proposed device is capable of capturing 0.8 mg of DOX with 200 μg or fabricated beads. Its small size with less than 2 cm length and 3.1 mm diameter enables this device to employed in small animal models and tested *in vivo.* Also, SF and ENCC can decrease toxicity of DOX on 3T3 fibroblast cells significantly, by increasing the cell viability from average 28% to 94% with indicate the effectiveness of these beads on capturing ability and reducing toxicity of DOX.

# References:


1. R. L. Siegel, K. D. Miller, A. Jemal, Cancer statistics, 2020. *CA: A Cancer Journal for Clinicians* **70**, 7-30 (2020).

2. K. Miller *et al.*, Cancer treatment and survivorship statistics. *CA Cancer J Clin* **65**, 271-289 (2012).

3. E. Frei III, G. P. Canellos, Dose: a critical factor in cancer chemotherapy. *The American Journal of Medicine* **69**, 585-594 (1980).

4. K. D. Miller *et al.*, Cancer treatment and survivorship statistics, 2016. *CA: A Cancer Journal for Clinicians* **66**, 271-289 (2016).

5. R. A. DePinho, The age of cancer. *Nature* **408**, 248 (2000).

6. M. Ferrari, Cancer nanotechnology: opportunities and challenges. *Nature Reviews Cancer* **5**, 161 (2005).

7. T. Finkel, M. Serrano, M. A. Blasco, The common biology of cancer and ageing. *Nature* **448**, 767 (2007).

8. Q. Hu, W. Sun, C. Wang, Z. Gu, Recent advances of cocktail chemotherapy by combination drug delivery systems. *Advanced Drug Delivery Reviews* **98**, 19-34 (2016).

9. J. M. Llovet *et al.*, Arterial embolisation or chemoembolisation versus symptomatic treatment in patients with unresectable hepatocellular carcinoma: a randomised controlled trial. *The Lancet* **359**, 1734-1739 (2002).

10. A. S. Patel *et al.*, Development and validation of endovascular chemotherapy filter device for removing high-dose doxorubicin: preclinical study. *Journal of Medical Devices* **8**, 041008 (2014).

11. W.-J. Hwu *et al.*, A clinical-pharmacological evaluation of percutaneous isolated hepatic infusion of doxorubicin in patients with unresectable liver tumors. *Oncology Research Featuring Preclinical and Clinical Cancer Therapeutics* **11**, 529-537 (1999).

12. C. M. Blumenfeld *et al.*, Drug capture materials based on genomic DNA-functionalized magnetic nanoparticles. *Nature Communications* **9**, 2870 (2018).

13. H. J. Oh *et al.*, 3D Printed Absorber for Capturing Chemotherapy Drugs before They Spread through the Body. *ACS Central Science* **5**, 419-427 (2019).

14. X. C. Chen *et al.* (2016) Copolymer membrane for high-dose chemotherapy delivery during transarterial chemoemblization. (Google Patents).

15. A. Sheikhi *et al.*, Modular microporous hydrogels formed from microgel beads with orthogonal thermo-chemical responsivity: Microfluidic fabrication and characterization. *MethodsX* **6**, 1747-1752 (2019).

16. J. M. de Rutte, J. Koh, D. Di Carlo, Scalable High-Throughput Production of Modular Microgels for In Situ Assembly of Microporous Tissue Scaffolds. *Advanced Functional Materials*, 1900071 (2019).

17. T. G. van de Ven, A. Sheikhi, Hairy cellulose nanocrystalloids: a novel class of nanocellulose. *Nanoscale* **8**, 15101-15114 (2016).

18. C. Yee *et al.*, Endovascular Ion Exchange Chemofiltration Device Reduces Off-Target Doxorubicin Exposure in a Hepatic Intra-arterial Chemotherapy Model. *Radiology: Imaging Cancer* **1**, e190009 (2019).

19. A. Sheikhi *et al.*, Microengineered Emulsion-to-Powder Technology for the High-Fidelity Preservation of Molecular, Colloidal, and Bulk Properties of Hydrogel Suspensions. *ACS Applied Polymer Materials* **1**, 1935-1941 (2019).

20. W. Xiao *et al.*, Synthesis and characterization of photocrosslinkable gelatin and silk fibroin interpenetrating polymer network hydrogels. *Acta Biomaterialia* **7**, 2384-2393 (2011).

21. D. N. Rockwood *et al.*, Materials fabrication from Bombyx mori silk fibroin. *Nature Protocols* **6**, 1612 (2011).

22. S. Chen, M. Liu, H. Huang, L. Cheng, H.-P. Zhao, Mechanical properties of Bombyx mori silkworm silk fibre and its corresponding silk fibroin filament: A comparative study. *Materials & Design* **181**, 108077 (2019).

23. H. Yang, D. Chen, T. G. van de Ven, Preparation and characterization of sterically stabilized nanocrystalline cellulose obtained by periodate oxidation of cellulose fibers. *Cellulose* **22**, 1743-1752 (2015).

24. B. Hofreiter, I. Wolff, C. Mehltretter, Chlorous Acid Oxidation of Periodate Oxidized Cornstarch2. *Journal of the American Chemical Society* **79**, 6457-6460 (1957).

25. H. Yang, M. N. Alam, T. G. van de Ven, Highly charged nanocrystalline cellulose and dicarboxylated cellulose from periodate and chlorite oxidized cellulose fibers. *Cellulose* **20**,

1865-1875 (2013).

26. S. Shah *et al.*, Fluorescence properties of doxorubicin in PBS buffer and PVA films. *Journal of Photochemistry and Photobiology B: Biology* **170**, 65-69 (2017).

27. N. S. H. Motlagh, P. Parvin, F. Ghasemi, F. Atyabi, Fluorescence properties of several chemotherapy drugs: doxorubicin, paclitaxel and bleomycin. *Biomedical Optics Express* **7**, 2400-2406 (2016).

28. S. Sugiura, M. Nakajima, S. Iwamoto, M. Seki, Interfacial tension driven monodispersed droplet formation from microfabricated channel array. *Langmuir* **17**, 5562-5566 (2001).

29. S. Wiedemeier *et al.*, Precision moulding of biomimetic disposable chips for droplet-based applications. *Microfluidics and Nanofluidics* **21**, 167 (2017).

30. Z. Li, A. Leshansky, L. Pismen, P. Tabeling, Step-emulsification in a microfluidic device. *Lab on a Chip* **15**, 1023-1031 (2015).

31. S. H. Kim, D. A. Weitz, One-step emulsification of multiple concentric shells with capillary microfluidic devices. *Angewandte Chemie International Edition* **50**, 8731-8734 (2011).

32. M. Tsukada, G. Freddi, P. Monti, A. Bertoluzza, N. Kasai, Structure and molecular conformation of tussah silk fibroin films: Effect of methanol. *Journal of Polymer Science Part B: Polymer Physics* **33**, 1995-2001 (1995).

33. Y. Kishimoto, H. Morikawa, S. Yamanaka, Y. Tamada, Electrospinning of silk fibroin from all aqueous solution at low concentration. *Materials Science and Engineering: C* **73**,

498-506 (2017).